



UNIVERSITY OF LEEDS

This is a repository copy of *Transcriptomic Analysis Reveals Prognostic Molecular Signatures of Stage I Melanoma*.

White Rose Research Online URL for this paper:
<http://eprints.whiterose.ac.uk/149276/>

Version: Supplemental Material

Article:

Thakur, R, Laye, JP, Lauss, M et al. (14 more authors) (2019) Transcriptomic Analysis Reveals Prognostic Molecular Signatures of Stage I Melanoma. *Clinical Cancer Research*, 25 (24). pp. 7424-7435. ISSN 1078-0432

<https://doi.org/10.1158/1078-0432.CCR-18-3659>

© 2019, American Association for Cancer Research. This is an author produced version of a journal article published in *Clinical Cancer Research*. Uploaded in accordance with the publisher's self-archiving policy.

Reuse

Items deposited in White Rose Research Online are protected by copyright, with all rights reserved unless indicated otherwise. They may be downloaded and/or printed for private study, or other acts as permitted by national copyright laws. The publisher or other rights holders may allow further reproduction and re-use of the full text version. This is indicated by the licence information on the White Rose Research Online record for the item.

Takedown

If you consider content in White Rose Research Online to be in breach of UK law, please notify us by emailing eprints@whiterose.ac.uk including the URL of the record and the reason for the withdrawal request.



eprints@whiterose.ac.uk
<https://eprints.whiterose.ac.uk/>

Supplementary Table and Figures

Supplementary table S1: Summary of the Cox proportional hazards model testing interaction between the Lund 2-grades and the AJCC stage

Variable (n=544, deaths=157)	Hazard ratio	95% CI*	P
Lund 2-grade: High-grade vs. Low-grade	0.9	0.4-2.2	0.9
AJCC stage II & III vs AJCC stage I	1.9	1.04-3.4	0.04
AJCC stage x Lund 2-grade (interaction)	2.7	1.0-6.9	0.04

*CI= Confidence interval

The significant interaction between the Lund 2-grade and AJCC stage implies that the effect of Lund 2-grade on risk of death was different across the AJCC stages. The low-grade from Lund 2-grade and AJCC stage I were chosen as the baseline groups where n is the total number samples and deaths are number of melanoma specific-deaths. The unclassified samples from the Lund 2-grade were excluded from the analysis.

Supplementary table S2: Summary of univariable Cox proportional hazard analysis for Gerami genes in the whole LMC dataset and in stage I subset

Gerami genes	Whole LMC dataset					Stage I subset				
	HR	95% CI		P	FDR	HR	95%CI		P	FDR
BAP1	1	0.9	1.2	0.6	0.6	0.9	0.7	1.2	0.51	0.94
MGP	1.1	0.9	1.3	0.2	0.3	0.9	0.6	1.3	0.57	0.94
SPP1	1.3	1.1	1.5	0.001	0.003	1.2	0.8	1.6	0.36	0.94
CXCL14	0.7	0.6	0.8	10⁻⁹	1x10⁻⁸	1.0	0.6	1.6	0.97	0.98
CLCA2	0.8	0.7	0.9	0.0002	0.0006	0.9	0.6	1.3	0.68	0.94
S100A8	0.8	0.7	0.9	0.009	0.01	0.9	0.6	1.3	0.63	0.94
BTG1	0.7	0.6	0.9	0.0001	0.0004	0.9	0.6	1.3	0.55	0.94
SAP130	1.0	0.9	1.2	0.8	0.9	0.9	0.8	1.1	0.18	0.94
ARG1	0.8	0.7	1.0	0.02	0.02	0.9	0.6	1.2	0.49	0.94
KRT6B	0.8	0.7	0.9	0.002	0.004	1.0	0.7	1.5	0.97	0.98
GJA1	0.7	0.6	0.8	5x10⁻⁷	4x10⁻⁶	0.7	0.5	1.0	0.05	0.94
ID2	0.7	0.7	0.8	6x10⁻⁸	7x10⁻⁷	0.8	0.7	1.1	0.15	0.94
EIF1B	1.3	1.1	1.5	0.001	0.003	1.0	0.8	1.4	0.85	0.98
S100A9	0.8	0.7	0.9	0.004	0.009	0.9	0.7	1.3	0.65	0.94
CRABP2	0.8	0.7	0.9	0.002	0.004	1.0	0.7	1.4	0.97	0.98
KRT14	0.8	0.7	0.9	0.0002	0.0005	1.0	0.6	1.6	0.98	0.98
ROBO1	0.9	0.8	1.0	0.005	0.01	0.9	0.7	1.1	0.28	0.94
RBM23	1.2	1.0	1.4	0.009	0.01	1.3	0.9	1.8	0.13	0.94
TACSTD	0.7	0.6	0.8	8x10⁻⁶	8x10⁻⁵	0.9	0.6	1.3	0.70	0.94
DSC1	0.8	0.7	0.9	0.001	0.003	1.1	0.8	1.6	0.61	0.94
SPRR1B	0.8	0.7	1.0	0.01	0.01	0.8	0.6	1.2	0.36	0.94
TRIM29	0.8	0.7	0.9	0.0003	0.0009	1.0	0.7	1.4	0.87	0.98
AQP3	0.8	0.6	0.9	0.0001	0.0005	0.9	0.6	1.3	0.55	0.94
TYRP1	0.9	0.8	1.1	0.4	0.4	1.2	0.8	1.8	0.43	0.94
PPL	0.7	0.6	0.8	2x10⁻⁵	0.0001	0.9	0.6	1.3	0.57	0.94
LTA4H	1.2	1.0	1.3	0.04	0.05	1.1	0.8	1.5	0.68	0.94
CST6	0.8	0.7	0.9	0.007	0.01	1.0	0.7	1.4	0.94	0.98

HR=hazards ratio, CI=confidence interval, FDR=false discovery rate.

Supplementary table S3: The consensus PAM clustering initially performed on 703 LMC tumors identified 8 classes. Two of the eight classes contained too few samples (1 and 15), which were identified as potentially outlying observations frequently observed to be present on the edges of the plate. Re-clustering after removing these samples (n=16) robustly confirmed the original 6 classes. The columns and rows in the table below contain the classification with and without outlying observations.

		Initial clustering						
		Class	1	2	3	4	5	6
Re-clustering after removing 16 samples	1	71	0	0	0	0	0	1
	2	0	122	0	0	0	1	3
	3	0	0	72	5	0	0	6
	4	0	0	1	135	0	0	0
	5	0	0	0	3	135	0	0
	6	0	0	0	0	0	0	132

Supplementary table S4: Univariable and multivariable analysis adjusting the AJCC stage of the LMC classes for melanoma-specific survival in the whole LMC dataset

Variable tested	Univariable				Multivariable		
	Category or unit	HR	95% CI ^a	P	HR	95% CI ^a	P
LMC class	1	1.0	-	-	1.0	-	-
	2	1.7	0.8 - 3.5	0.1	0.8	0.3 - 1.9	0.8
	3	5.0	2.5 - 10.1	7×10⁻⁶	3.2	1.5 - 6.8	0.003
	4	2.4	1.2 - 4.7	0.01	2.0	0.9 - 4.2	0.05
	5	1.5	0.7 - 3.1	0.2	1.5	0.7 - 3.3	0.3
	6	3.1	1.6 - 6.1	0.001	2.0	1.0 - 4.2	0.05
AJCC stage	I	1.0	-	-	1.0	-	-
	II	2.4	1.6 - 3.6	9×10⁻⁶	1.8	1.1 - 2.8	0.01
	III	5.9	3.8 - 9.0	9×10⁻¹⁶	5.3	3.2 - 8.7	1.4×10⁻¹⁰
Sex	F	1.0	-	-	1.0	-	-
	M	1.5	1.1 - 1.9	0.007	1.3	0.9 - 1.8	0.1
Age at diagnosis	years	1.03	1.01 - 1.04	5×10⁻⁶	1.03	1.02 - 1.05	1.7×10⁻⁵
Mitotic rate	Count per mm ²	1.1	1.0 - 1.5	1×10⁻⁹	1.1	1.0-1.1	0.0003

CI= confidence interval, HR= Hazards ratio

Supplementary table S5: Univariable analysis of LMC classes for melanoma-specific survival in the LMC stage I subset

LMC Class	HR	95% CI	P
1	1.0	-	-
2	4.1	0.8 - 19.6	0.08
3	3.7	0.5 – 26.0	0.2
4	3.2	0.6 – 15.3	0.2
5	2.2	0.4 – 10.3	0.3
6	6.6	1.4 – 31.2	0.02

CI=confidence interval, HR=hazards ratio

Supplementary table S6: Multivariable analysis of LMC classes for melanoma-specific survival in the whole LMC dataset and LMC stage I tumors adjusting histological variables

Variable tested	Whole LMC dataset				LMC stage I		
	Category or unit	HR	95% CI	P	HR	95% CI	P
LMC class	1	1.0	-	-	1.0	-	-
	2	1.0	0.4 - 2.3	1.0	6.8	0.7-62.6	0.09
	3	3.0	1.4 - 6.6	0.005	5.1	0.3-86.4	0.3
	4	2.1	1.0 - 4.4	0.05	6.2	0.7-54.1	0.09
	5	1.5	0.7-3.1	0.3	3.9	0.5-32.6	0.2
	6	2.0	0.9-4.1	0.06	9.8	1.1-86.2	0.04
Sex	F	1.0	-	-	1.0	-	-
	M	1.4	0.9-1.9	0.06	2.7	1.1-6.7	0.04
Ulceration status	No	1.0	-	-	1.0	-	-
	Yes	1.4	1.0-2.1	0.04	0.4	0.05-4.1	0.5
Age at diagnosis	years	1.03	1.01-1.04	3x10⁻⁴	1.01	0.98-1.1	0.4
Mitotic rate	Count per mm ²	1.04	0.99-1.08	0.06	1.3	1.0-1.5	0.01
Breslow thickness	mm	1.1	1.1-1.2	7x10⁻⁵	1.1	0.3-3.5	0.9

CI=confidence interval, HR=hazards ratio

Supplementary table S7: Summary of univariable and bivariable Cox proportional hazards model analysis for Gerami clusters and the LMC classes in the whole LMC dataset

Signature		Univariable			bivariable		
		HR	95% CI	P	HR	95% CI	P
LMC classes	Class 1	1.0	-	-	1.0		
	Class 2	1.7	0.8 - 3.5	0.1	1.7	0.8 - 3.5	0.1
	Class 3	5.0	2.5 - 10.1	7×10⁻⁶	4.1	2.0 - 8.3	0.0001
	Class 4	2.4	1.2 - 4.7	0.01	2.4	1.2 - 4.9	0.01
	Class 5	1.5	0.7 - 3.1	0.2	1.8	0.9 - 3.8	0.1
	Class 6	3.1	1.6 - 6.1	0.001	2.7	1.4 - 5.4	0.003
Gerami clusters	Cluster 1	1.0	-	-	1.0	-	-
	Cluster 2	0.5	0.4 - 0.6	5×10⁻⁷	0.6	0.4 - 0.8	0.003

CI= confidence interval, HR=hazards ratio. The Gerami clusters were generated after clustering the tumours using expressions of the 27 Gerami genes with the same clustering algorithm as for the generation of the LMC classes. In this analysis of the whole dataset the two signatures show additive (i.e. independent) effects.

Supplementary table S8: Summary of univariable and bivariable Cox proportional hazards models for Gerami clusters and the LMC classes in Stage I group

Signature		Univariable			bivariable		
		HR	95% CI	P	HR	95% CI	P
LMC classes	Class 1	1.0	-	-	1.0	-	-
	Class 2	4.1	0.8 - 19.6	0.08	4.2	0.9 - 20.5	0.07
	Class 3	3.7	0.5 - 26.0	0.2	3.2	0.4 - 23.5	0.2
	Class 4	3.2	0.6 - 15.3	0.2	3.3	0.7 - 15.7	0.1
	Class 5	2.2	0.4 - 10.3	0.3	2.4	0.5 - 11.7	0.3
	Class 6	6.6	1.4 - 31.2	0.02	6.6	1.4 - 31.2	0.02
Gerami clusters	Cluster 1	1.0	-	-	1.0	-	-
	Cluster 2	0.6	0.3 - 1.4	0.3	0.7	0.3 - 1.6	0.4

CI=confidence interval, HR=hazards ratio, n is the number of samples. In this analysis of stage I melanomas, only our new signature shows a prognostic effect in both univariable and bivariable analyses.

Supplementary table S9: Replicating the LMC signature in the Lund primary melanoma cohort
(Relapse-free survival)

Lund primary melanoma cohort (n=200, relapsers=75)			
LMC Class	Hazard ratio	95% CI	P
1	1.0	-	-
2	1.5	0.4-5.5	0.5
3	6.3	3.1-12.9	6 × 10⁻⁷
4	4.2	1.7-10.1	0.001
5	1.1	0.4-3.0	0.8
6	3.7	1.6-8.4	0.002

CI=confidence interval, n= number of samples and relapsers are the number of cases with a relapse.

Supplementary table S10: SNB status (performed or not performed) breakdown by T stage for LMC patients (mucosal samples unused in survival analyses are not included)

T-stage	SNB no	SNB yes	Total
T0	3	0	3
T1a	10	1	18
T1b	30	9 &	31
T2a	136	74	210
T2b	20	19	40
T3a	90	61	152
T3b	54	42	96
T4a	29	19	48
T4b	57	26	82
Total	429	251	680

& Among these T1b stage patients, 7 were SNB negative and they were subsequently re-staged to IA according to guidelines.

Supplementary table S11: Life table summary for patients who underwent SNB and were followed up for melanoma specific survival

Time post-diagnosis (years)	Patients who died from melanoma (A)	Patients censored (B)	Patients alive (C)	Patients informative for survival analysis (D= A+C)	Total (D+B)
1	4	1	235	239	240
2	18	7	215	233	240
3	29	40	171	200	240
4	35	72	133	168	240
5	40	89	111	151	240
6	51	109	80	131	240
7	52	136	52	104	240
8	54	148	38	92	240

Supplementary table S12: AJCC stage pre-SNB and post-SNB for patients who had a SNB and were followed up for melanoma-specific survival (n=240)

AJCC stage pre-SNB	AJCC stage post-SNB					
	IA	IB	IIA	IIB	IIC	III
IA	0	0	0	0	0	1
IB	7	60	0	0	0	13
IIA	0	0	62	0	0	15
IIB	0	0	0	38	0	20
IIC	0	0	0	0	14	10

Supplementary table S13: Clinico-histological comparison between patients who did vs. those who did not undergo SNB

Clinico-histological characteristic	Stage III patients				Whole LMC			
	Clinical stage III (N=44)	SNB-confirmed stage III (N=65)	Univariable P-value	Multivariable P-value [§]	No SNB (N=436)	SNB performed (N=251)	Univariable P-value	Multivariable P-value ^{§§}
Year of Diagnosis (%)								
2000 - 2005	74.3	25.7	7x10 ⁻⁷	4x10 ⁻⁶	86.2	13.8	3x10 ⁻³⁸	2x10 ⁻²⁸
2006 - 2012	24.3	75.7			38.6	61.4		
Age at diagnosis (yrs)	61.4 (32.1, 78.6)	57.1 (28.5, 74.7)	0.13	0.11	58.3 (18.3, 81.3)	59.0 (19.6, 76.8)	0.92	
Sex (% male)	54.6	36.9	0.07	0.61	45.5	44.6	0.82	
Tumor site (% limbs)	34.1	44.6	0.27		40.7	43.8	0.42	
Breslow thickness in mm (median, range)	4 (1.1, 12)	3 (1, 10)	0.05	0.30	2.2 (0.3, 20.0)	2.3 (0.8, 10.0)	0.24	
Ulcerated (%)	47.7	43.1	0.63		32.2	35.1	0.44	
BMI (%) [§]								
<25	22.5	40.3	0.09	0.17	36.5	36.7	0.26	
25-30	35.0	35.5			37.0	42.0		
>30	42.5	24.2			26.5	21.2		
Deprivation score (median and range) ^{&}	-0.6 (-3.3, 9.0)	-1.1 (-4.2, 11.1)	0.28		-0.7 (-4.5, 12.0)	-1.3 (-4.6, 16.5)	10 ⁻³	0.04
Smoking (% ever smoked)	61.5	46.7	0.15	0.45	52.6	43.6	0.03	0.40
Use of statins or aspirin [^]	34.1	29.0	0.58		21.1	23.8	0.42	

[§]BMI: body mass index (kg/m²)

[&]Level of deprivation as indicated by the Townsend score derived from residence postcode. Higher score indicates more deprivation.

[^]Regular use of statins (anti-cholesterol) and aspirin (anti-hypertension) were included as a putative measure of the level of comorbidities (22% of the cohort).

[§]Logistic regression modelling jointly all factors with a significant or suggestive association from the univariable analysis ($P \leq 0.15$ used given limited power)

^{§§} Logistic regression modelling jointly all factors with a significant association in the univariable analysis ($P \leq 0.05$)

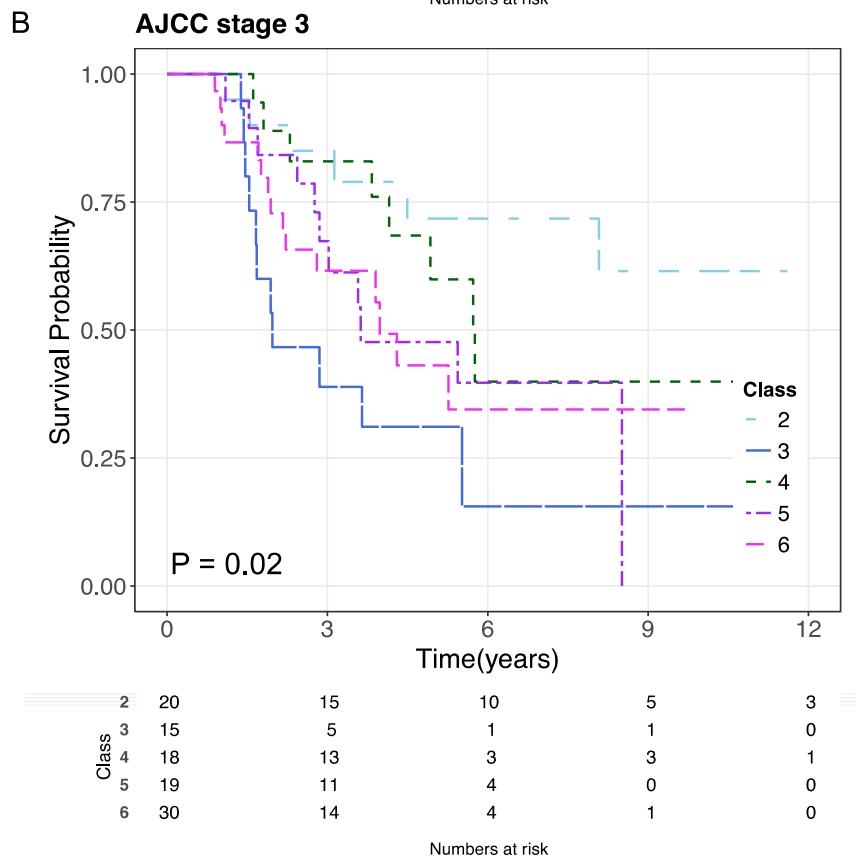
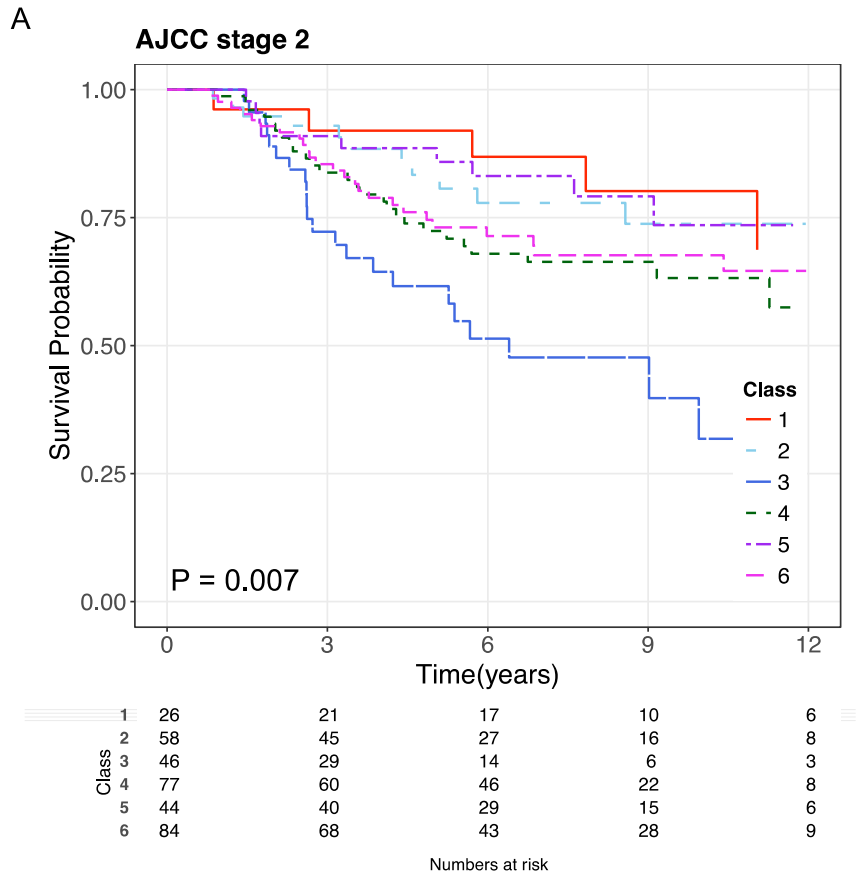
Supplementary table S14: Summary of up- and down-regulated biological pathways in the six classes of LMC signature

Broad category	Pathways	Class 1	Class 2	Class 3	Class 4	Class 5	Class 6
Immune	Hematopoietic cell lineage(K)	↑ 1.1×10^{-14}		↓ 2.2×10^{-14}	↓ 1.9×10^{-4}		
	Natural killer cell mediated cytotoxicity(K)	↑ 1.1×10^{-14}		↓ 1.6×10^{-10}	↓ 2.1×10^{-7}		
	TNF signaling pathway(K)	↑ 8.4×10^{-12}		↓ 3.6×10^{-14}	↓ 1.9×10^{-4}		
	T cell receptor signaling pathway(K)	↑ 9.6×10^{-14}		↓ 2.2×10^{-9}	↓ 1.8×10^{-8}		
	Jak-STAT signaling pathway(K)	↑ 3.1×10^{-10}		↓ 3.8×10^{-6}	↓ 2.9×10^{-3}		
	Fc epsilon RI signaling pathway(K)	↑ 2.7×10^{-8}		↓ 7.3×10^{-6}	↓ 7.0×10^{-4}		
	NOD-like receptor signaling pathway(K)	↑ 9.8×10^{-5}		↓ 4.6×10^{-5}			
	Toll-like receptor signaling pathway(K)	↑ 3.6×10^{-9}		↓ 2.3×10^{-5}	↓ 7.2×10^{-4}		
	Osteoclast differentiation(K)	↑ 1.1×10^{-14}		↓ 2.2×10^{-14}	↓ 1.8×10^{-7}		
	NF-kappa B signaling pathway(K)	↑ 1.1×10^{-14}		↓ 4.4×10^{-14}	↓ 1.6×10^{-5}		
	Chemokine signaling pathway (K)	↑ 1.1×10^{-14}			↓ 5.1×10^{-6}		
	B cell receptor signaling pathway(K)	↑ 2.5×10^{-10}			↓ 2.3×10^{-6}	↓ 7.5×10^{-6}	
Antigen processing and presentation(K)	↑ 2.3×10^{-7}			↓ 2.0×10^{-6}	↓ 2.4×10^{-3}		
Cell growth and death	Apoptosis(K)	↑ 1.1×10^{-8}		↓ 1.9×10^{-4}			
	Cell cycle(K)	↓ 4.0×10^{-6}	↓ 4.2×10^{-3}	↑ 1.8×10^{-4}			↑ 1.9×10^{-3}

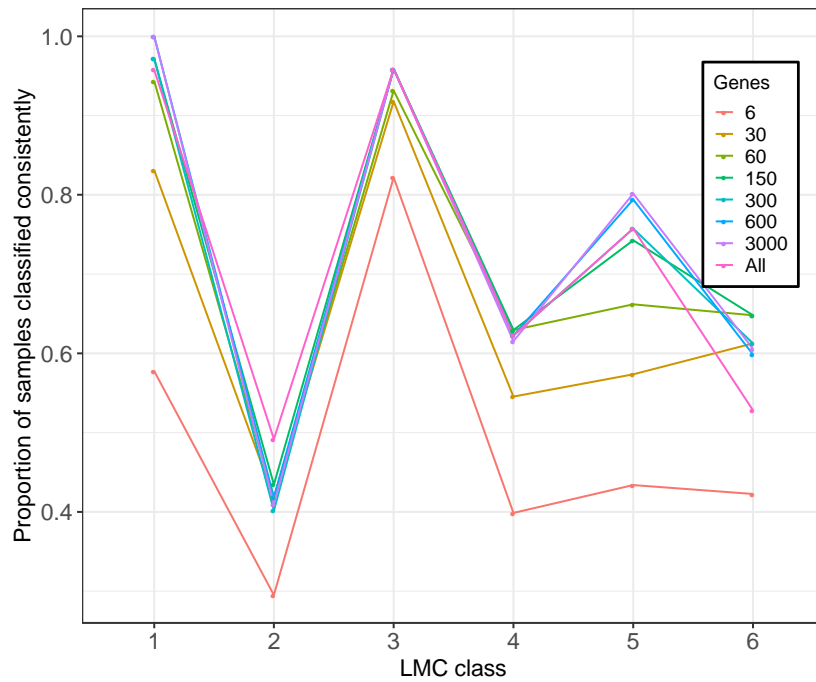
Cell communication and motility	Axon guidance(K)		↓ 1.8×10^{-3}		↑ 1.2×10^{-3}	
	ECM-receptor interaction(K)		↓ 3.6×10^{-7}		↑ 2.5×10^{-4}	↑ 2.1×10^{-3}
	Rap1 signaling pathway(K)	↑ 6.6×10^{-6}	↓ 7.3×10^{-6}		↑ 2.9×10^{-3}	↓ 3.7×10^{-3}
	Focal adhesion(K)	↑ 5.3×10^{-5}	↓ 7.1×10^{-8}		↑ 5.1×10^{-3}	↑ 1.6×10^{-3}
	Regulation of actin cytoskeleton(K)	↑ 3.3×10^{-3}	↓ 4.6×10^{-4}	↓ 5.5×10^{-3}		↓ 3.9×10^{-3}
	Cell adhesion molecules (CAMs)(K)	↑ 2.1×10^{-8}	↓ 6.6×10^{-8}	↓ 8.8×10^{-4}		
	Assembly of the primary cilium(R)		↑ 1.0×10^{-8}	↑ 7.0×10^{-4}	↓ 2.4×10^{-5}	
Signal transduction	Ras signaling pathway(K)	↑ 3.3×10^{-5}	↓ 3.5×10^{-5}		↑ 1.7×10^{-3}	
	Hippo signaling pathway(K)				↑ 1.3×10^{-3}	
	PI3K-Akt signaling pathway(K)	↑ 4.3×10^{-6}	↓ 4.3×10^{-7}		↑ 2.8×10^{-3}	
	TCF dependent signaling in response to WNT(R)		↑ 1.9×10^{-3}			
	MAPK signaling pathway(K)	↑ 3.2×10^{-7}	↓ 2.3×10^{-6}	↓ 1.7×10^{-4}		
Cell metabolism	Selenoamino acid metabolism(R)		↑ 2.2×10^{-9}	↑ 2.5×10^{-3}		↓ 1.4×10^{-14}
	Eukaryotic Translation Initiation(R)		↑ 2.3×10^{-12}	↑ 2.1×10^{-4}		↓ 1.4×10^{-14}
	Nonsense-Mediated Decay (NMD)(R)		↑ 2.2×10^{-9}			↓ 1.4×10^{-14}
	Eukaryotic Translation Termination(R)		↑ 1.4×10^{-10}	↑ 2.5×10^{-3}		↓ 1.4×10^{-14}

SRP-dependent cotranslational protein			
targeting to membrane(R)	$\uparrow 2.5 \times 10^{-10}$	$\uparrow 3.6 \times 10^{-4}$	$\downarrow 1.4 \times 10^{-14}$
Eukaryotic Translation Elongation(R)	$\uparrow 2.7 \times 10^{-10}$	$\uparrow 3.7 \times 10^{-3}$	$\downarrow 1.4 \times 10^{-14}$

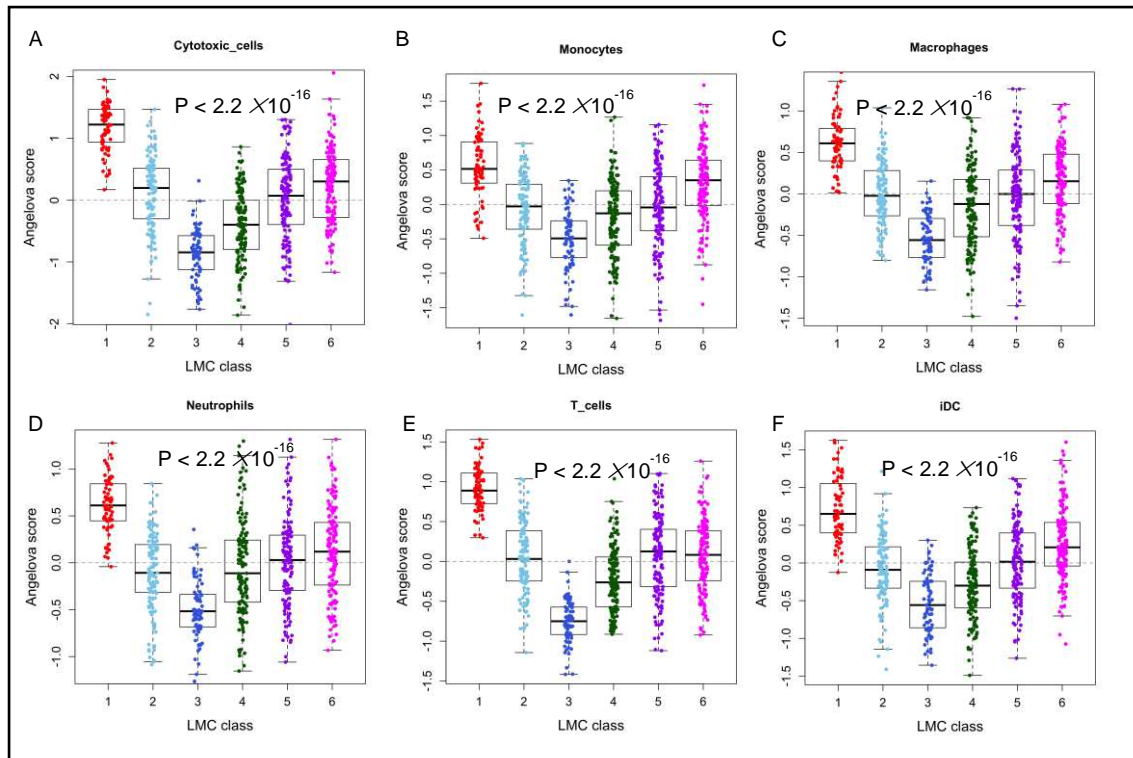
The hypergeometric test P-values (after FDR correction) for enrichment in up- and downregulated pathways are indicated with \uparrow and \downarrow respectively. ECM stands for extracellular matrix.



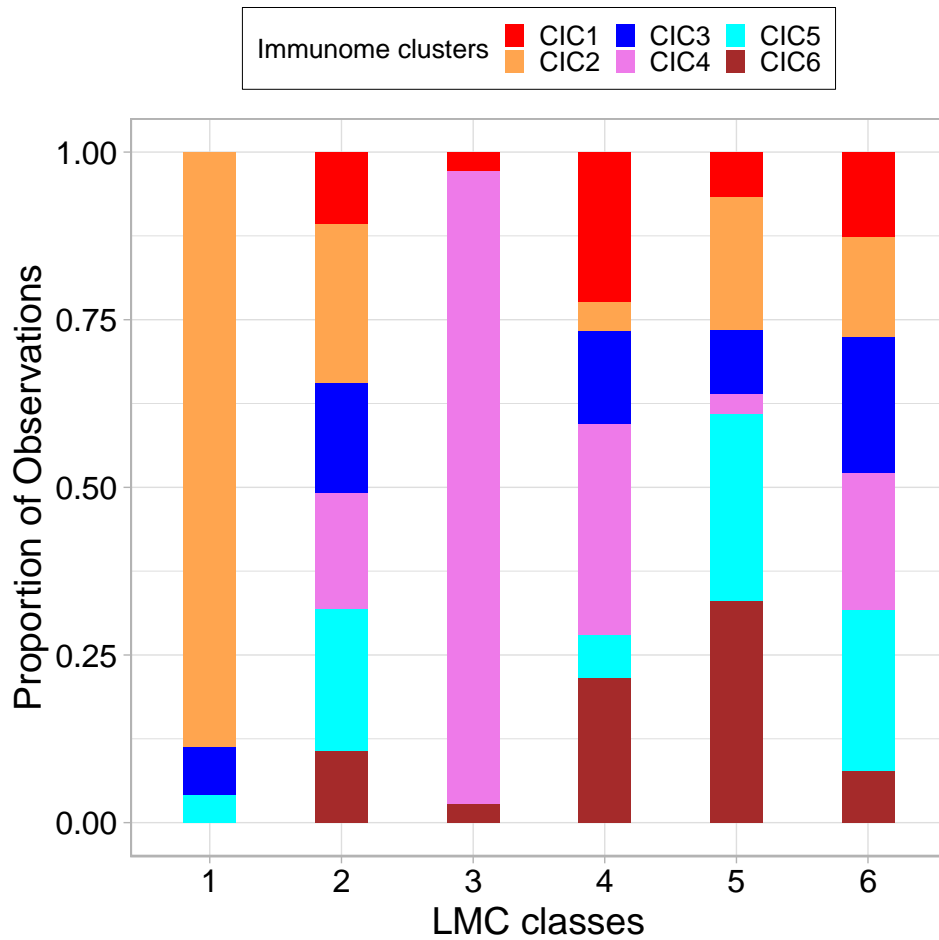
Supplementary figure S1: Melanoma-specific survival for LMC classes within AJCC stages 2 and 3.



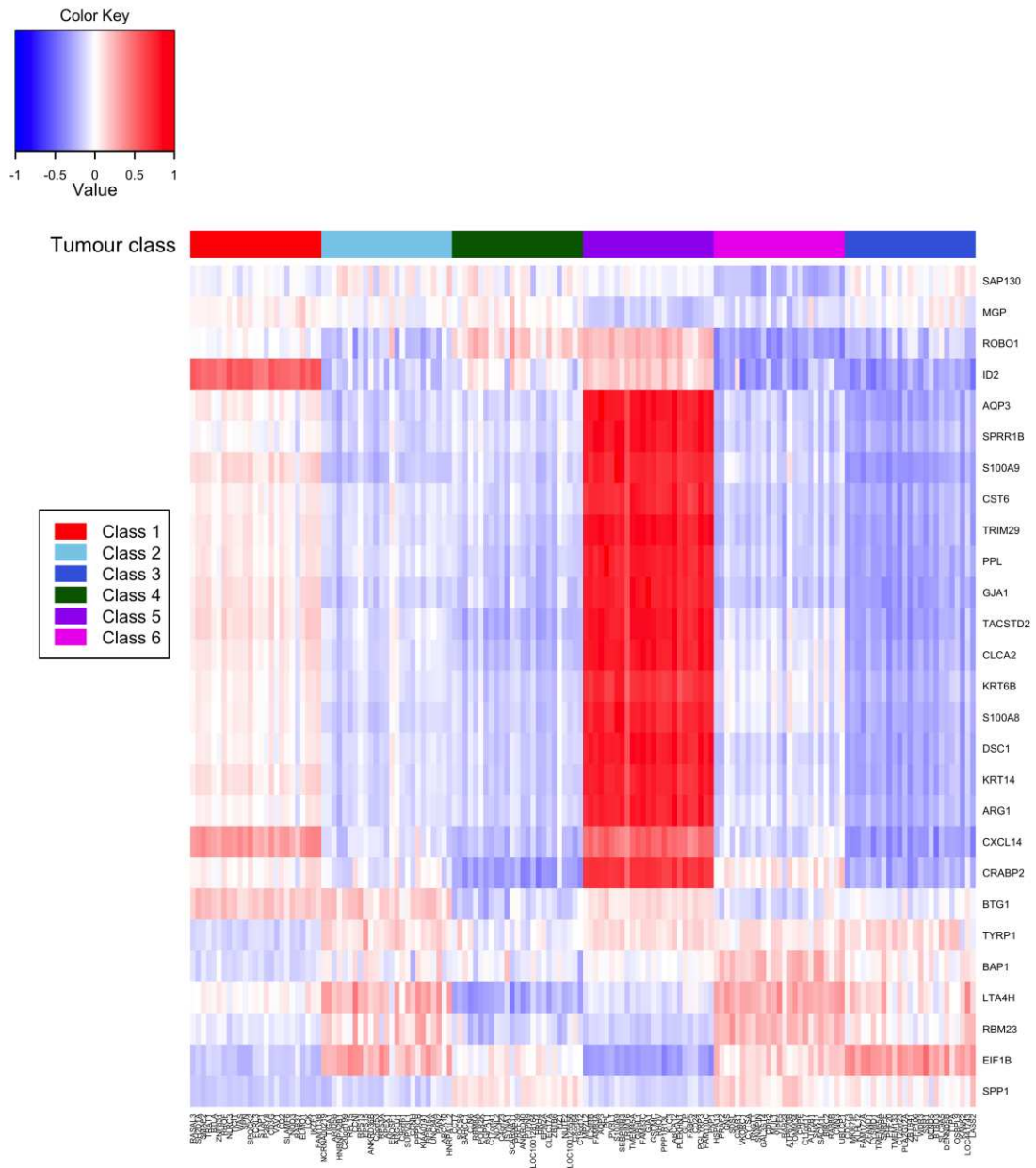
Supplementary figure S2: Refining the initial LMC signature comprising of 13,688 genes. Six gene signatures were generated by combining the top y (1, 5, 10, 25, 50 and 100) most differentially upregulated genes in each LMC class (giving the signature total of 6, 30, 60, 150, 300 and 600 genes). The class centroids for the signatures were calculated as the average expression of those top genes within the class. The LMC tumors were reclassified into the six classes of LMC signature using the NCC approach. As a comparison baseline, the initial signature reclassified the tumors in their correct classes with 50-100% accuracy (mean= 67%). Signatures derived from the top 6, 30, and 60 differentially expressed genes (1, 5, and 10 per class) showed substantially decreased accuracy in one or more classes while the gene signature comprising 150-600 genes (top 25-100 from each class) showed very little drop in accuracy. We retained the signature of 150 genes as the final refined signature (top 25 upregulated genes within each LMC class).



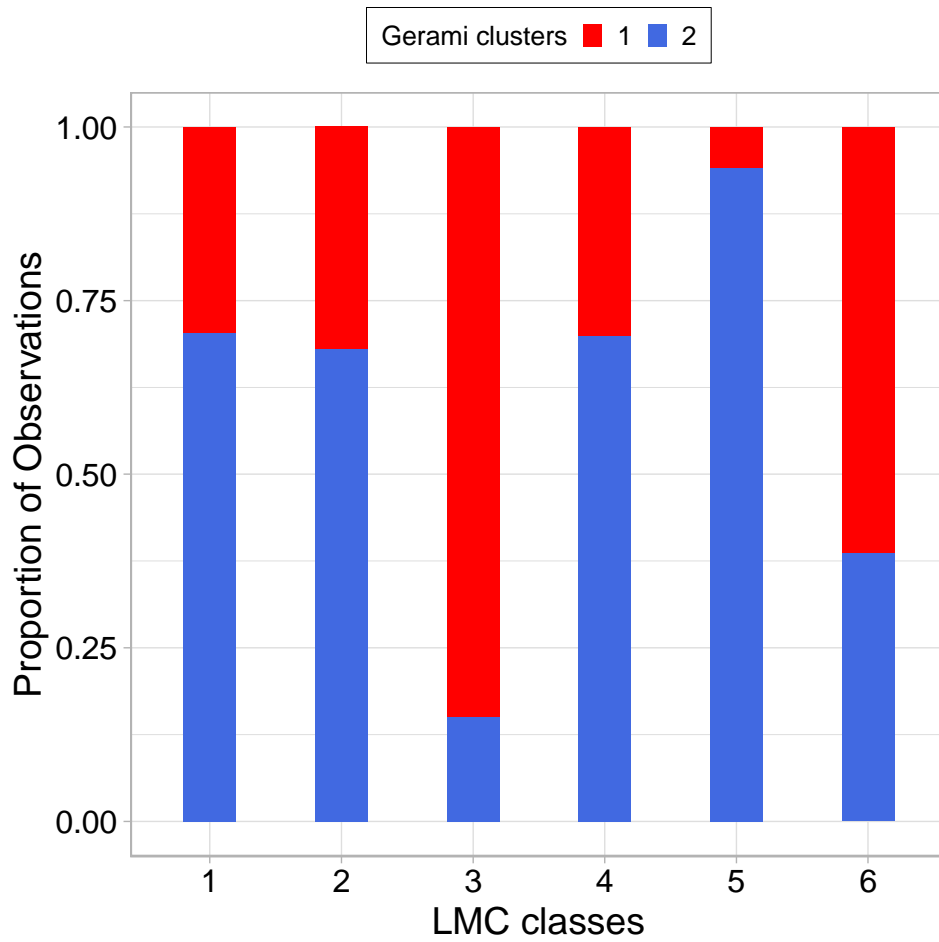
Supplementary figure S3: Immune cell score-based characterization of the classes in LMC signature. The immune cell scores (Angelova score) were derived from a list of genes reported to be specifically associated with various immune cell types. (A-F) The dot and boxplots show the distributions of score for the key immune cell types among the 27 scored (Pvalue from Kruskal-Wallis test with Bonferroni correction).



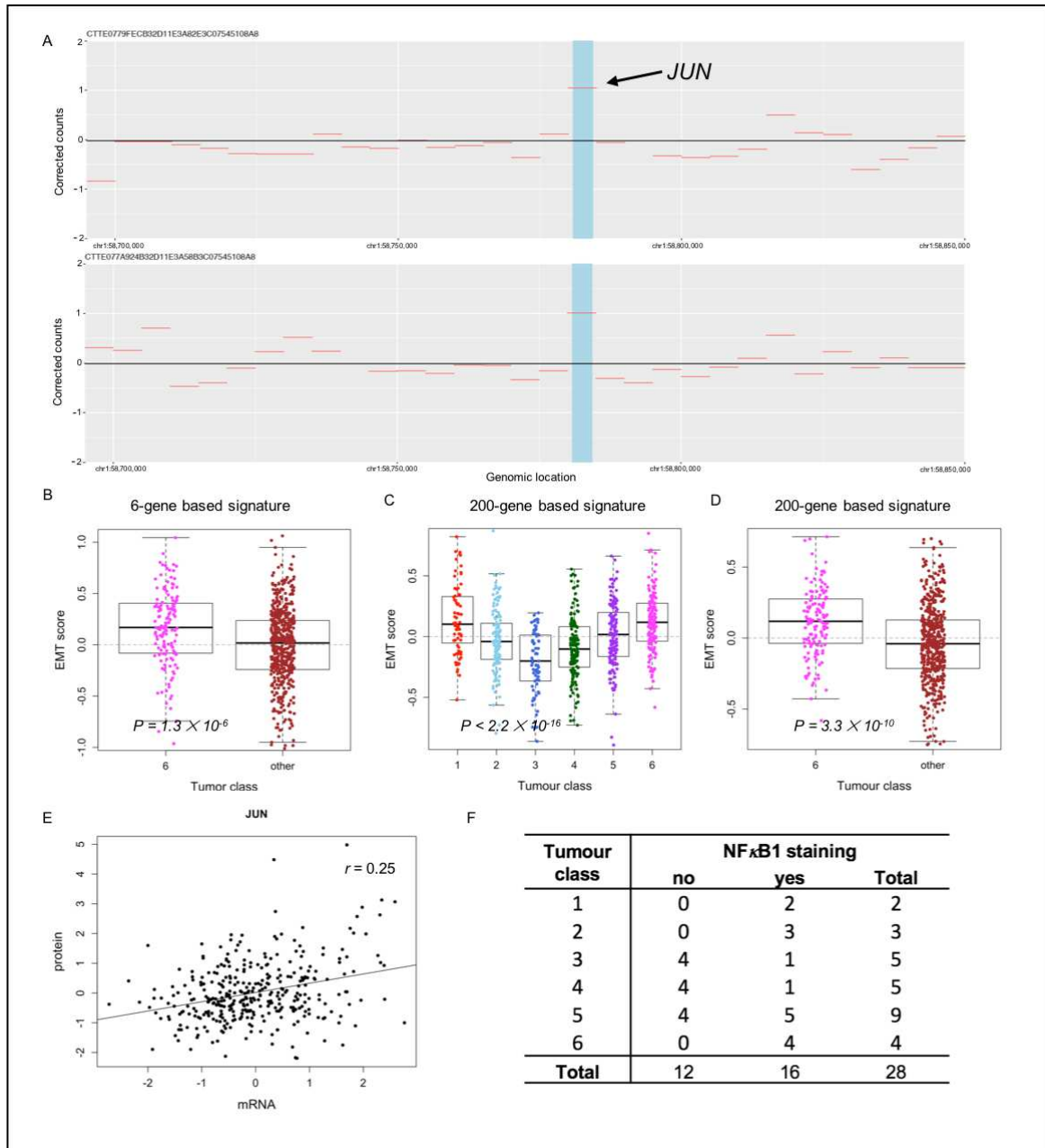
Supplementary figure S4: Overlap between Consensus Immunome Clusters (CIC) and LMC classes in the whole LMC dataset. LMC class 3 (worst prognosis) overlaps with CIC4 (weakest immune profile) and LMC class 1 (best survival) matched CIC2 (strongest immunological profile). Other LMC classes had little to no overlap with the CICs, reflecting that they are likely driven by non-immunological pathways.



Supplementary figure S5: Heatmap of correlation between Gerami genes (rows) and LMC signature genes (columns) in the whole LMC dataset. The blue color in the heatmap represents negative correlation while red represents positive correlation. The LMC signatures genes were ordered based on their expression across the LMC classes. Gerami genes had their strongest correlation with LMC classes 5 and 3.



Supplementary figure S6: Overlap between the Gerami clusters and LMC classes in the whole LMC dataset. The Gerami cluster 1 closely matched the LMC class 3 tumors while Gerami cluster 2 overlapped with LMC class 5 tumors.



Supplementary figure S7: Biological profiling of the LMC class 6 tumors. (A) An example of JUN copy number gains in two tumour samples from class 6. (B-D) LMC class 6 association with scores of epithelial to mesenchymal transition (EMT) pathway based on 6 and 200-genes (Pvalues from Mann-Whitney U test or Kruskal-Wallis test). (E) Correlation between JUN mRNA and protein expression in the TCGA dataset. (F) Summary of immunohistochemistry staining for NF-κB1 across the 6 LMC classes.